ACS OMEGA

http://pubs.acs.org/journal/acsodf

Article

Unsaturated Vinyl-Type Carbocation $[(CH_3)_2C{=}CH]^+$ in Its Carborane Salts

Evgenii S. Stoyanov,* Irina Yu. Bagryanskaya, and Irina V. Stoyanova

Cite This: *ACS Omega* 2021, 6, 15834–15843

Read Online

ACCESS | Metrics & More | Article Recommendations | Supporting Information

ABSTRACT: The isobutylene carbocation $(CH_3)_2C{=}CH^+$ was obtained in amorphous and crystalline salts with the carborane anion $CHB_{11}Cl_{11}^-$. The cation was characterized by X-ray crystallography and IR spectroscopy. Its crystal structure shows a relatively uniform ionic interaction of the cation with the surrounding anions, with a slightly shortened distance between the C atom of the =CH group and the Cl atom of the anion, pointing to a higher positive charge on this group. In the amorphous phase, the asymmetric interaction of the cation with the anion increases, approaching ion pairing. This gives rise to a strong hyperconjugation between the two CH_3 groups and the $2p_z$ orbital of the central carbon sp^2 atom (the red shift of the CH stretch is 150 cm^{-1}); this effect stabilizes the cation. Over time, as the structure of the amorphous phase becomes more ordered, the hyperconjugation weakens and disappears in the crystalline phase with the disappearance of ion pairing. The carbocation stabilization in the crystalline phase is achieved due to the transfer of a portion of the charge to the neighboring anions, whereas the charge on the C=C bond becomes the strongest: the C=C stretch frequency drops to ~160 cm^{-1} relative to neutral isobutylene. The collected IR spectra for the optimized cation under vacuum (in the 6-311G ++ (d, p) basis for all HF, MP2, and DFT calculations) predict that a positive charge on the C=C bond increases its stretching frequency; this computational result contradicts the experimental data, perhaps because it does not take into account the significant impact of the environment.

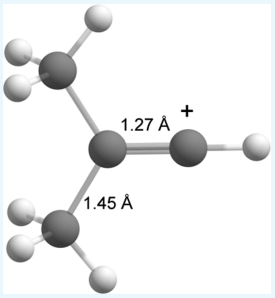

1. INTRODUCTION

Unsaturated carbocations containing C=C or C≡C bonds are known only for the species containing electron-donor groups, which contribute to the stabilization of the cation because of the distribution of positive charge over them. The examples are carbocations containing phenyl[1,2] or anthracene[3] groups, vinyl-type carbocations $R'C^+{=}CR''_2$ (with R′= cyclopropyl or *t*-Bu and R″= *β*-silyl),[4−6] and carbocations with other electron-donating groups.[7−9] The research on carbocations with *β*-silyl groups has drawn investigators' attention because the silylium ions R_3Si^+ behave similarly to protons as substituents.[10,11] This state of affairs should bring the properties of such carbocations closer to those of the vinyl type not stabilized by heteroatoms or electron-donating groups. The *β*-silyl-substituted vinyl cations $R'C^+{=}CR''_2$ with R′= cyclopropyl and *t*-Bu have been characterized by X-ray crystallography.[4,5] It was found that increased localization of the positive charge onto the C=C bond leads to its shortening and an unusual high-frequency shift of the $C{=}C^+$ stretching vibration (up to 1958 cm^{-1}), indicating that the bond order for this linkage is markedly higher than 2. In other words, an increase in the positive charge on the C=C bond causes an increase in the electron density on it. If vinyl cations do not contain electron-donating alkyl substituents (cyclopropyl or *t*-Bu) and even *β*-silyl groups, such as allyl $C_3H_5^+$ and butylene $C_4H_7^+$ cations, then the positive charge on the C=C bond is significantly higher. It is interesting whether this feature further enhances these unusual properties of the C=C bond. This knowledge is important for a deeper understanding of the properties of the double CC bond.

Nonstabilized vinyl- or allyl-type carbocations are believed to be very unstable because the accumulation of a high positive charge on the C=C bond results in high reactivity toward all accessible nucleophiles. Such carbocations have not been studied in detail because their salts in pure form have not yet been obtained. The simplest and least stable $C_2H_3^+$ and $C_3H_5^+$ cations have been studied experimentally only under vacuum by mass-selected IR spectroscopy.[12,13] The most stable isomer of the $C_2H_3^+$ ion under vacuum has a nonclassic bridged proton structure with the bridging proton stretch vibration at 2158 cm^{-1}; the C=C stretch frequency has not been determined. The classic Y-shaped isomer of $C_2H_3^+$ is expected to form in a condensed phase and has not been obtained and investigated experimentally. The $C{=}C^+$ stretch vibration of the $CH_3{-}C^+{=}CH_2$ cation under vacuum has been detected at 1877 cm^{-1} by IR photodissociation spectroscopy.[13] This value is lower than the corresponding frequencies for stabilized vinyl cations of the $R'C^+{=}CR_2''$ type, and this observation does not confirm the proposed tendency for the frequency to increase

Received: March 10, 2021
Accepted: June 1, 2021
Published: June 10, 2021

with the increasing positive charge on the C=C bond. Numerous attempts have been made to study the allyl cation, $C_3H_5^+$, by NMR spectroscopy in liquid superacids at low temperature, and they have failed.[14] Formation of $C_3H_5^+$ has been proved in a cryogenic superacidic matrix (170 K) by IR spectroscopy.[15,16] With the increasing temperature up to 230 K, the IR spectrum of the sample changes. Thus, it is expected that nonstabilized alkene carbocations are stable only at low temperatures (below −100° C), and their salts in pure form have not yet been obtained.

In this work, we report the results of a study on the salts of isobutylene carbocation $(CH_3)_2C{=}CH^+$ with the positive charge localized mainly on the C=C bond; the salts were analyzed in amorphous and crystalline phases by IR spectroscopy and X-ray crystallography at room temperature. As a counterion, the undecachlorocarborane anion, $CHB_{11}Cl_{11}^-$, was chosen. Its extreme stability and very low basicity promote the formation of stable salts with highly reactive cations.[17]

2. RESULTS

Sublimation of carborane acid, $H(CHB_{11}Cl_{11})$ (hereafter abbreviated as $H\{Cl_{11}\}$), on cold Si windows of an IR cell reactor leads to the formation of a thin translucent layer yielding an intense IR spectrum. Injection of gaseous 1,2-dichloro-2-methylpropane (DCMP) into the IR cell caused a surface reaction with the acid with the release of HCl, whose adsorption appeared in the IR spectrum. This reaction generates a mixture of products because the solid acid is polymeric[18] and its interaction with adsorbed molecules proceeds through depolymerization, which slows down the first stage of the reaction

$$H\{Cl_{11}\} + C_4H_8Cl_2 \rightarrow C_4H_8Cl\{Cl_{11}\} + HCl$$

The initially formed compound has time to participate in subsequent reactions, thereby complicating the study. For this reason, instead of the pure acid, its salt $CH_2Cl\{Cl_{11}\}$ was used. It reacts quickly with DCMP, allowing the early stages of the reaction to be analyzed with fewer complications caused by side reactions.

Salt $CH_2Cl\{Cl_{11}\}$ is formed by the reaction

$$H\{Cl_{11}\} + CH_2Cl_2 \rightarrow CH_2Cl^+\{Cl_{11}^-\} + HCl \quad (1)$$

Its preparation is described in the Experimental Section. For further discussion, it is important to show in Figure 1 the slope of the linear dependence of absorption intensity of the formed HCl (measured at 2821 cm^{-1}) on the intensity of the 3063 cm^{-1} band of the formed CH_2Cl^+ cation in accordance with eq 1.

The interaction of DCMP with the $CH_2Cl\{Cl_{11}\}$ salt on the Si windows of the IR cell was monitored by recording IR spectra at short intervals. The absorption bands of the CH_2Cl^+ cation were found to decrease and disappear, and a spectrum of a new cationic product and the characteristic spectra of gaseous dichloromethane (DCM; bands at 1267 and 759 cm^{-1}) and HCl appeared. The formation of DCM is possible if the CH_2Cl^+ cation interacts with DCMP as a dechlorinating agent according to the equation

$$CH_2Cl^+ + C_4H_8Cl_2 \rightarrow CH_2Cl_2 + C_4H_8Cl^+ \quad (2)$$

to form a monochlorocarbocation. The dependence of the decrease in the intensity of the CH_2Cl^+ cation spectrum on an increase in the absorption corresponding to gaseous DCM

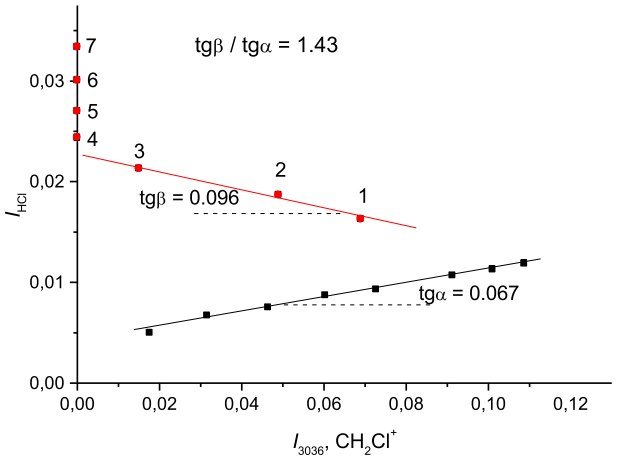

Figure 1. Dependence of HCl formation on the formation/consumption of the CH_2Cl^+ cation according to the intensities of the H−Cl stretch at 2821 cm^{-1} (I_{HCl}) and of the CH stretch of the CH_2Cl^+ cation at 3036 cm^{-1} (in a.u.).

(measured at 1267 cm^{-1}) is linear, thus confirming their relation in accordance with eq 2. The simultaneous emergence of HCl absorption indicates that the monochlorocarbocation, $C_4H_8Cl^+$, rapidly decays into unsaturated carbocation $C_4H_7^+$ (eq 3)

$$C_4H_8Cl^+ \rightarrow C_4H_7^+ + HCl \quad (3)$$

If the reaction proceeds only according to eqs 2 and 3, then the slope of the dependence of the absorption intensities of the formed HCl on consumed CH_2Cl^+ should match that for the formed HCl and CH_2Cl^+, according to eq 1. This is because the latter corresponds to molar ratio $HCl/CH_2Cl^+ = 1$. Nonetheless, the ratio of the two slopes is 1.43 (Figure 1). This means that, simultaneously with reaction 3, a further reaction of the interaction of $C_4H_7^+$ with DCMP proceeds with the release of HCl and the formation of another cationic product, which we will designate as A^+

$$C_4H_7^+ + DCMP \rightarrow A^+ + HCl \quad (4)$$

The spectra of cations $C_4H_7^+$ and A^+ formed before the completion of CH_2Cl^+ consumption show three bands in the frequency range of C=C stretch vibrations: at 1555 and 1540 cm^{-1} and a wide and intense band at ~1495 cm^{-1} (Figures 2 and S2). As CH_2Cl^+ is consumed, the intensities of these bands increase approximately equally (spectra 1−4 in Figures 1 and 2); that is, cations $C_4H_7^+$ and A^+ are formed in approximately equal molar amounts. After consumption of CH_2Cl^+, if the reaction is not stopped by vacuum removal of DCMP vapors, then the formation of HCl continues (Figure 1, spectra 5−7). In this case, the band at 1555 cm^{-1} decreases, while the bands at 1540 and 1495 cm^{-1} increase (Figure 2). It can be assumed that the band at 1555 cm^{-1} belongs to the $C_4H_7^+$ cation, whose interaction with DCMP gives rise to the A^+ cation with bands at 1540 and 1495 cm^{-1}. If we subtract the spectrum with more intense absorption of the A^+ cation (spectrum 7) from the spectrum of the mixture of cations $C_4H_7^+$ and A^+ (spectrum 4) until absorption of A^+ is completely subtracted, then we can isolate the spectrum of the $C_4H_7^+$ cation with a symmetric band at 1555 cm^{-1} (Figure 3, red, and Figure S5 in the Supporting Information). The reverse subtraction of the spectra makes it possible to isolate the A^+ spectrum (Figures 3 and S6 in the Supporting Information).

https://doi.org/10.1021/acsomega.1c01297
ACS Omega 2021, 6, 15834−15843

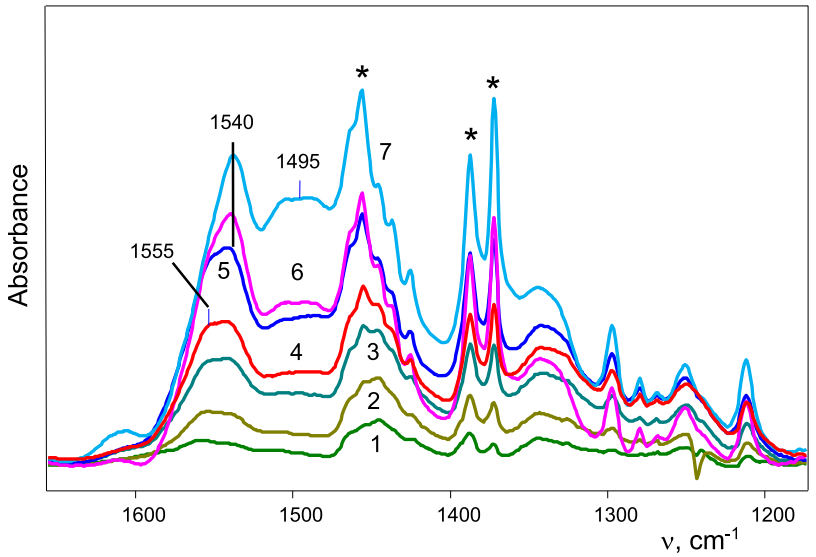

Figure 2. Overlapping IR spectra of cations $C_4H_7^+$ and A^+ and adsorbed DCMP molecules (marked with asterisks). The spectra of gaseous DCMP and DCM are subtracted.

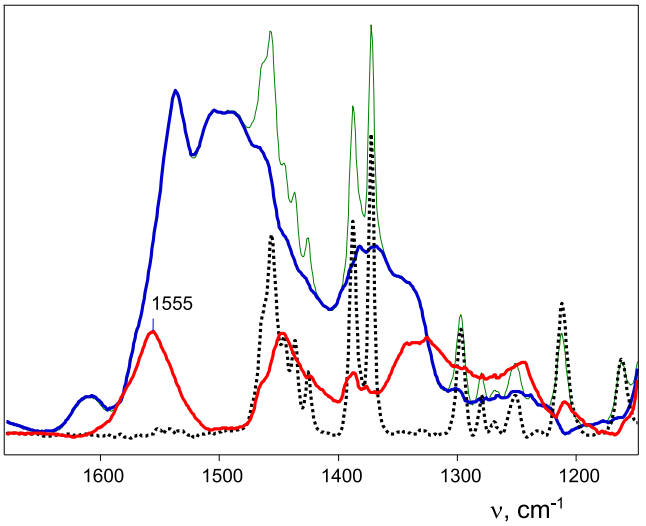

Figure 3. IR spectra of cation $C_4H_7^+$ (red) isolated by subtracting spectrum 7 from spectrum 4 (for details, see Figure S2 in the Supporting Information) and cation A^+ (blue) obtained by reverse subtraction (7 − 4; green), followed by subtraction of the spectrum of adsorbed DCMP (dotted line).

The IR spectra of cations also contain the bands of adsorbed DCMP. Its spectrum was obtained as follows. The removal of DCMP vapors from the reactor cell containing a film of carbocation salts on Si windows by blowing with argon led to the emergence of intense bands of adsorbed DCMP in the spectrum of the sample. If the cell was further evacuated (down to 5×10^{-5} ppm), then the adsorbed DCMP was partially removed, and the intensity of its absorption weakened. Subtracting the second spectrum from the first revealed the spectrum of adsorbed DCMP (Figures 3 and S4 in the Supporting Information). Its frequencies are close to those of gaseous DCMP, with the exception of the CCl stretch at the tertiary C-atom: its frequency (633 cm^{-1}) diminished by 11 cm^{-1} as compared to free molecules.[19] That is, the adsorbed molecules solvated cations by attaching to them via their mostly basic site, the Cl atom at the *tert*-carbon. Repetitive recording of the spectrum of the sample with adsorbed DCMP molecules showed a rapid decrease in the intensity of their bands with time. After 50 min, they almost disappeared. Simultaneously, the absorption of the $C_4H_7^+$ cation decreased while that of A^+ increased accompanied by the appearance of HCl absorption. These data clearly show how the interaction of $C_4H_7^+$ with DCMP proceeds through the stage of solvation

$$C_4H_7^+ + C_4H_8Cl_2 \rightarrow C_4H_7^+ \cdot C_4H_8Cl_2 \xrightarrow[-HCl(-2HCl)]{} \underset{\text{cation } A^+}{C_4H_7 \cdot S^+},$$

where S = C_4H_7Cl or C_4H_6

Subtraction of the spectrum of adsorbed DCMP molecules from the spectra of solvated cations $C_4H_{7solv}^+$ and A_{solv}^+ allows us to isolate the spectra of bare $C_4H_7^+$ and A^+ cations (Figure 3). Unfortunately, we were unable to determine with proper accuracy whether one or two HCl molecules are released during the decomposition of the $C_4H_7^+ \cdot C_4H_8Cl_2$ solvate into the A^+ cation or to reliably analyze the number of Cl atoms in the A^+ cation (in the presence of 11 Cl atoms in the counterion).

Cations $C_4H_7^+$ and A^+ were also obtained through direct interaction of DCMP with the $H\{Cl_{11}\}$ acid. To the powder of the acid, a small amount of liquid DCMP was added such that its attenuated total reflectance (ATR) IR spectrum showed, besides the spectrum of the newly formed carbocation salts, the spectrum of the unreacted acid whose intensity corresponded to 20−50 mol % $H\{Cl_{11}\}$. The IR spectrum of the resulting product in the frequency range 1200−1700 cm^{-1} corresponds to a mixture of salts of cations $C_4H_7^+$ and A^+ formed in the gas cell reactor. By subtraction of the spectrum of the sample with a higher proportion of A^+ relative to $C_4H_7^+$ from the spectrum of the sample with a higher proportion of $C_4H_7^+$ relative to A^+, the spectrum of the $C_4H_7^+$ cation was isolated (Figure 4, red). In the frequency range 1200−1700 cm^{-1}, it is very close to the spectrum of the $C_4H_7^+$ cation formed in a gas cell (Figure 4, green). Nevertheless, there were differences in the frequency range of stretching CH vibrations, which are discussed below.

To determine the structure of carbocations, the method of X-ray structural analysis was used.

https://doi.org/10.1021/acsomega.1c01297
ACS Omega 2021, 6, 15834−15843

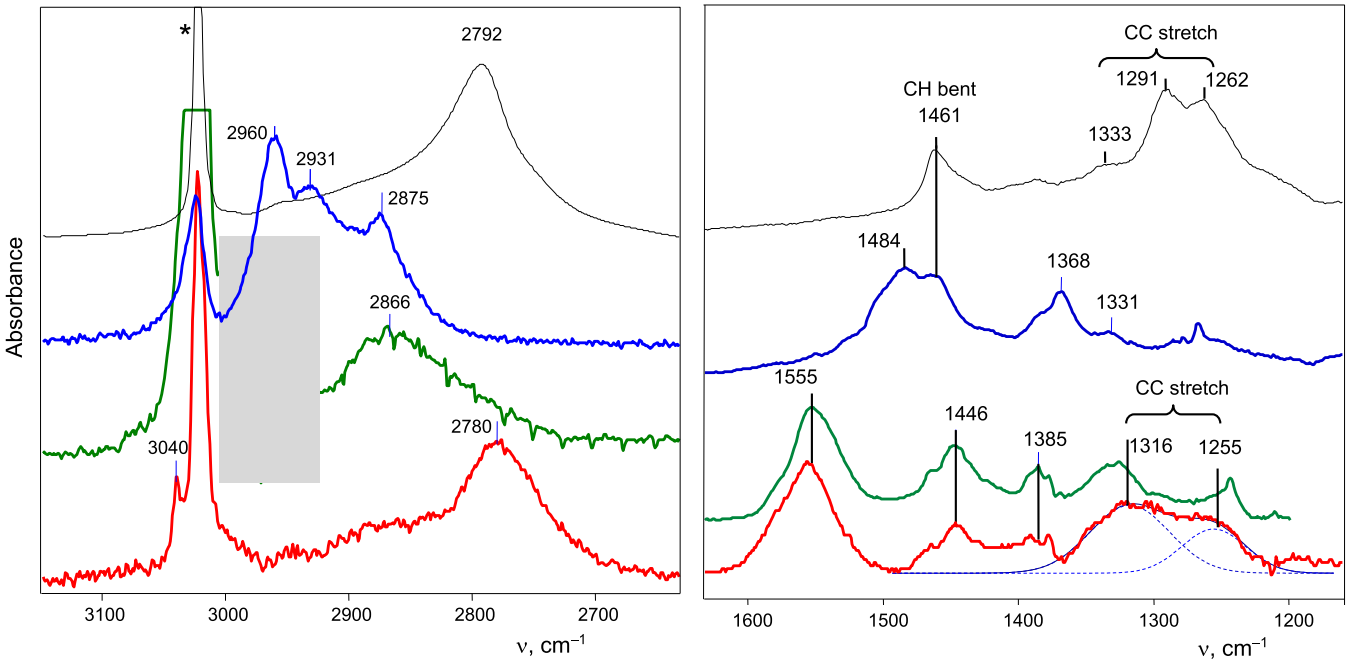

Figure 4. IR spectra of the $C_4H_7^+$ cation obtained by rapid interaction of H{Cl_{11}} with liquid DCMP (red) and by slow interaction with DCMP vapors (green, the spectrum contains remnants after subtraction of HCl adsorption) and also in a single crystal of $C_4H_7^+\{Cl_{11}^-\}$ (blue). The spectrum of *tert*-Bu^+ in the $C_4H_9^+\{Cl_{11}^-\}$ crystal is also given for comparison (black). The region of subtraction of strong bands is shaded; the CH stretch of the anion is marked with an asterisk.

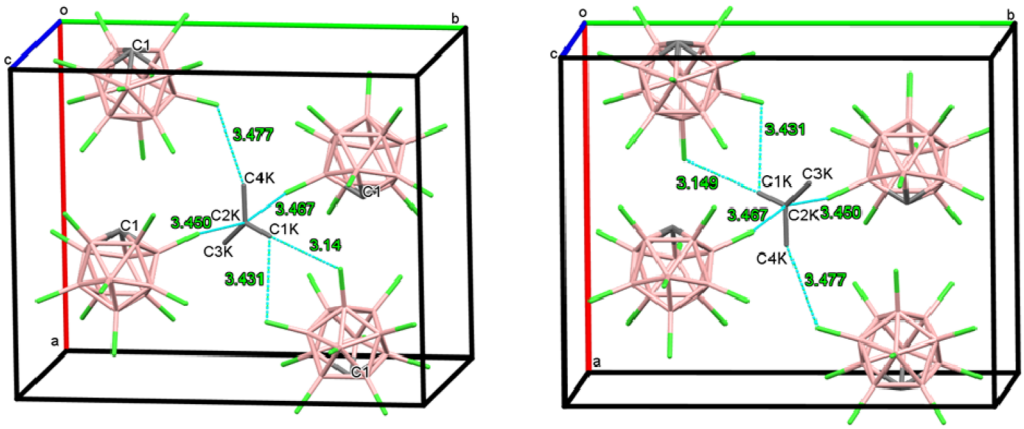

Figure 5. Two orientations of the isobutylene cation in the crystal lattice of the $C_4H_7^+\{Cl_{11}^-\}$ salt.

A mixture of salts of cations $C_4H_7^+$ and A^+ obtained upon completion of the reaction of dichlorobutane with CH_2Cl^+ (with spectrum 4 in Figures 1 and 2) was dissolved in DCM and was kept over hexane vapor. After a while, colorless crystals grew. The X-ray structure of the single crystals revealed that this is a salt of $C_4H_7^+\{Cl_{11}^-\}$ with discrete cations and anions. In the crystal lattice, the $C_4H_7^+$ cations have two orientations in which they interact identically with the surrounding anions (Figure 5). Superposition of cation structures in two orientations made it more difficult to determine the coordinates of carbon atoms (enlarged thermal ellipsoids). This disorder increased standard deviations of all geometric parameters of the cation (Tables S2 and S3 in the Supporting Information). Nevertheless, the shape of the cation was clear, which made it possible to determine its main structural features (Figure 6): it is flat with two identical and close-to-single CC bonds and one shortened CC bond. The CCC angles varied from 110 to 130°. In other words, this is an

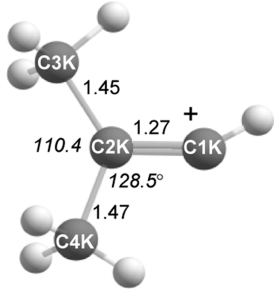

Figure 6. Structure of the cation in $C_4H_7^+\{Cl_{11}^-\}$ according to X-ray data (CC distances are expressed in Å and angles in degree).

isobutenyl cation, $(CH_3)_2C{=}CH^+$, with a distinct double C=C bond.

Considering the interaction of this cation with neighboring anions, it should be taken into account that the basicity of Cl

https://doi.org/10.1021/acsomega.1c01297
ACS Omega 2021, 6, 15834−15843

atoms in the $CHB_{11}Cl_{11}^-$ anion is different and decreases in the series "c" > "b" > "a" (Figure 7). In the crystal lattice, the carbon atom of the =CH group of the cation is directed at the most basic "c"-Cl atom of the anion, forming the shortest C···Cl separation of 3.14 Å (Figure 5). It is shorter than the sum of van der Waals radii r_C and r_{Cl} (3.53 Å),[20] thus forming a stronger H-bond with the anion than the CH_3 groups (these groups of the saturated *t*-Bu^+ carbocation formed relatively strong H-bonds with the $\{Cl_{11}^-\}$ counterions[21]). The H atom deviates slightly from the line connecting atoms C1K and Cl5 with a shortest distance of 3.14 Å: the C1K−H−Cl5 angle is 156.90° (Figure 8). The H bonding changes the H−C1K−C2K angle from 180° for the naked cation under vacuum to 168.8°. Thus, the =CH fragment is the most acidic and positively charged.

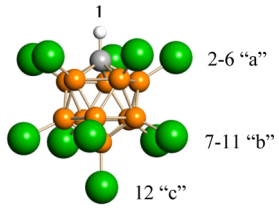

Figure 7. Icosahedral carborane anion $CHB_{11}Cl_{11}^-$ with the numbering of the three types of Cl atoms differing in basicity ("c" > "b" > "a").

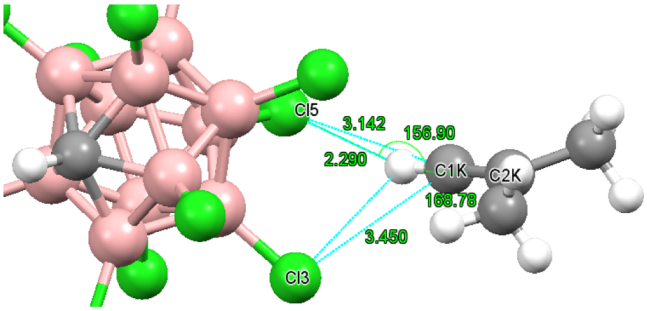

Figure 8. Preferential interaction of the isobutylene carbocation with one of the anions in the crystalline salt (coordinates of the H atoms were calculated).

If the salts of carbocations with an increasing proportion of cation A^+ were dissolved in dichloroethane, then the yield of the crystalline phase decreased until termination, and attempts to obtain crystals with cation A^+ failed. Crystallization of $C_4H_7^+\{Cl_{11}^-\}$ was accompanied by the formation of a waxy product. Its IR spectrum showed that it contains the A^+ cation and does not contain $C_4H_7^+$.

The $C_4H_7^+\{Cl_{11}^-\}$ crystals handpicked for recording of IR spectra were found to always be spotted with a waxy product. Therefore, the ATR IR spectrum of a crystal crushed on a diamond always contained a weak spectrum of a waxy product that had to be subtracted. The ATR IR spectrum of the crystal is shown in Figure 4 and in all frequency regions in Figure S7 in the Supporting Information.

2.1. Calculations. The optimized neutral isobutene molecule at the three levels of theory HF, MP2, and DFT gave very similar results (Table S4 in the Supporting Information), and the frequencies of their calculated IR spectra correlated well with those of the experimental one of gaseous isobutene (Figure 9). When the isobutenyl cation was optimized, the energy minimum was reached only in the HF calculation. Its IR spectrum does not contain imaginary frequencies and shows a good correlation with the spectrum of the cation in the crystalline salt for all frequencies, except for the C=C stretch, which exceeds the experimental value by ~150 cm^{-1} (Figure 10).

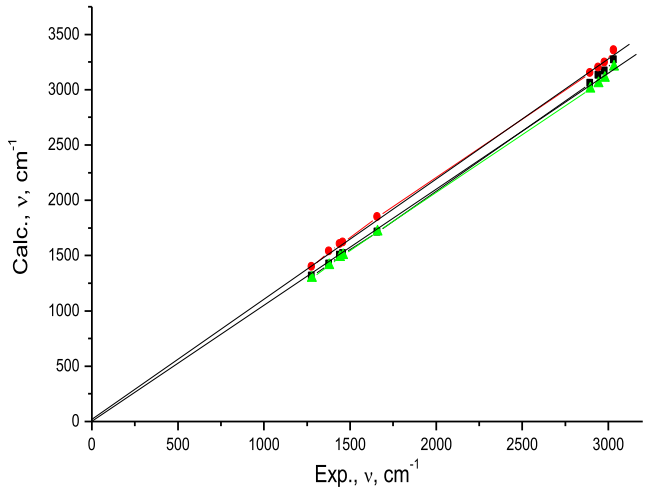

Figure 9. Correlation between calculated frequencies of isobutene optimized in HF (red), MP2 (black), and DFT (green) level and experimental frequencies for gaseous isobutene.[26]

Optimization of the isobutylene cation in the MP2 and DFT level was not achieved. When we searched for the minimum of the energy, the geometry of the cation changed, transforming it into a thermodynamically more stable linear isomer $CH_3-CH{=}C^+-CH_3$; however, this is the isobutenyl isomer that exists in the crystal phase. Probably, the crystal lattice promoted its stability.

The transfer of $C_4H_7^+$ from vacuum to a condensed phase should affect the distribution of its electron density owing to its solvation by neighboring anions and the influence of bulk properties of the condensed phase. For the saturated *t*-Bu^+ cation, we found[21] that electron perturbations imposed by the IEF-PCM continuum solvation model are minor: the CH stretches are decreased by 11−15 cm^{-1} at most. The IR spectrum of the *t*-Bu^+ cation calculated via the dielectric polarized continuum solvation model (D-PCM), which takes into account the electrostatic and dispersion−repulsion terms, actually showed similar minor changes in the frequencies of CH stretches (although the experimental change in the *t*-Bu^+ IR spectrum owing to the influence of the environment of the condensed phase is very significant[21]). For this reason, we did not carry out a quantum-chemical analysis of the bulk effects' influence on the unsaturated isobutylene carbocation.

Solvation is expected to have a stronger impact on the $C_4H_7^+$ cation. We simulated the solvation of isobutylene$^+$ by 13 Ar atoms under vacuum with the same crystallographic coordinates as those of the nearest chlorine atoms of the surrounding $\{Cl_{11}^-\}$ anions with C···Cl distances up to 3.5 Å (Figure S8 in the Supporting Information). The choice of neutral Ar atoms is based on the fact that their basicity is very close to that of the Cl atoms of $\{Cl_{11}^-\}$ anions in the crystal lattice.[22] Structure optimization for the isobutylene isomer in such a fixed environment again led to its transition to linear isomer $CH_3-CH{=}C^+-CH_3$ (Figure S8 in the Supporting

https://doi.org/10.1021/acsomega.1c01297
ACS Omega 2021, 6, 15834−15843

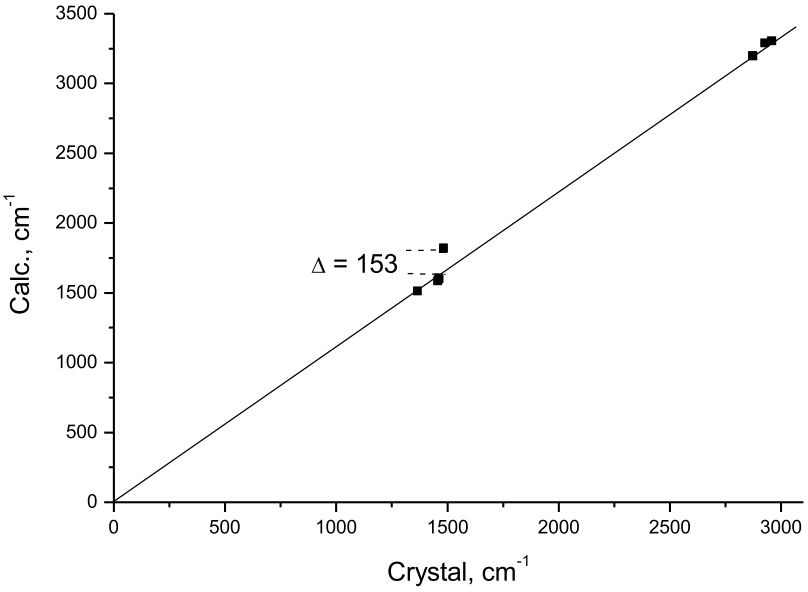

Figure 10. Correlations between calculated frequencies of the bare isobutylene cation at the HF level of theory and experimental frequencies of the $C_4H_7^+\{Cl_{11}^-\}$ crystal.

Information). Thus, according to calculations, the solvation of $C_4H_7^+$ by a weakly basic environment simulating $\{Cl_{11}^-\}$ anions is insufficient to stabilize the isobutylene isomer, in contradiction to experiment.

3. DISCUSSION

Scheme 1 shows five isomers (with the exception of two cyclic ones) that the $C_4H_7^+$ cation can form.

Scheme 1. Isomers of the $C_4H_7^+$ Cation (without Cyclic Forms)

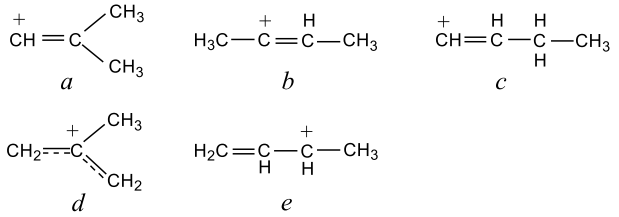

Their thermal stability increases in the series b, c, d, and e.[23−25] Our calculations show that isomer b is more stable than isobutylene cation a. That is, isobutylene is the least stable isomer of the $C_4H_7^+$ cation under vacuum. At the same time, X-ray analysis revealed that it is the isobutenyl cation that the salt $C_4H_7^+\{Cl_{11}^-\}$ contains. Quantum-chemical calculations at MP2/6-311G++(d,p) and B3LYP-D3/6-311G++(d,p) levels predict that even when surrounded by 13 Ar atoms mimicking the nearest Cl atoms of neighboring $\{Cl_{11}^-\}$ anions, whose basicity in the crystal lattice is close to that of the Ar atoms,[22] isobutylene should convert to b (Figure S8 in the Supporting Information). Thus, the application of quantum-chemical calculations to the study of vinyl cations in a solid phase has some limitations.

A comparison of the experimental IR spectrum of the isobutenyl cation in its crystalline salt with the experimental IR spectrum of gaseous isobutene[26] shows that there is a good correlation between their CH stretch and bent vibrations of the CH_3 groups (Figure 11). This allows us to empirically interpret the CH vibrations of the cation, which are consistent with those that follow from the calculations (Table 1). The slope of the correlation line (~1.005) is very close to 1.0, which means that the charge is insignificantly distributed over the CH_3 groups of the cation, without causing their polarization (a slight decrease in the frequencies of the CH stretch for the crystal phase is comparable to that observed when the molecules transition from the gaseous to the condensed phase). Therefore, the "+" charge of the cation is concentrated mainly on the double C═C bond, lowering its frequency by 160 cm^{-1}.

The Hartree−Fock calculation overestimates the frequency of the C═C stretch of the isobutenyl cation by 150 cm^{-1}, that is, almost equates it to neutral isobutene. The DFT calculation overestimates this frequency even more, by 360 cm^{-1}. This means that the emergence of the charge on the double C═C bond should lead to an increase, not a decrease, in its frequency by 200 cm^{-1}, in comparison with the neutral isobutene molecule. These results clearly illustrate limitations of quantum-chemical calculations in the research on alkene carbocations in the solid phase.

The spectrum of the amorphous salt of $C_4H_7^+$ that formed at the first instant of DCMP interaction with the $H\{Cl_{11}\}$ powder in the IR cell reactor differs from that of the crystalline salt: its C═C stretch is greater by 70 cm^{-1} and two new broad bands appear at 1316 and 1255 cm^{-1} (Figure 4). The latter are very close in frequency to the $CC(H_3)$ bonds of the *t*-Bu^+ cation (at 1330−1262 cm^{-1})[23] having one-and-a-half-bond status due to the involvement of CH_3 groups in hyperconjugation. The CH stretches of $C_4H_7^+$ also shares high similarity with that of *t*-Bu^+ (Figure 4), showing an intense broad low-frequency band at 2780 cm^{-1} (for *t*-Bu^+, it is located at 2791 cm^{-1}), which is highly characteristic for CH_3 groups involved in hyperconjugation with the empty $2p_z$ orbital of the central sp^2 carbon atom. The presence of such an empty orbital at the C1K atom of the cation is unexpected.

After a short period (1−2 min), the spectrum of amorphous $C_4H_7^+\{Cl_{11}^-\}$ changed in a specific way: absorption of CH vibrations increased to 2866 cm^{-1} and broadened greatly,

https://doi.org/10.1021/acsomega.1c01297
ACS Omega 2021, 6, 15834−15843

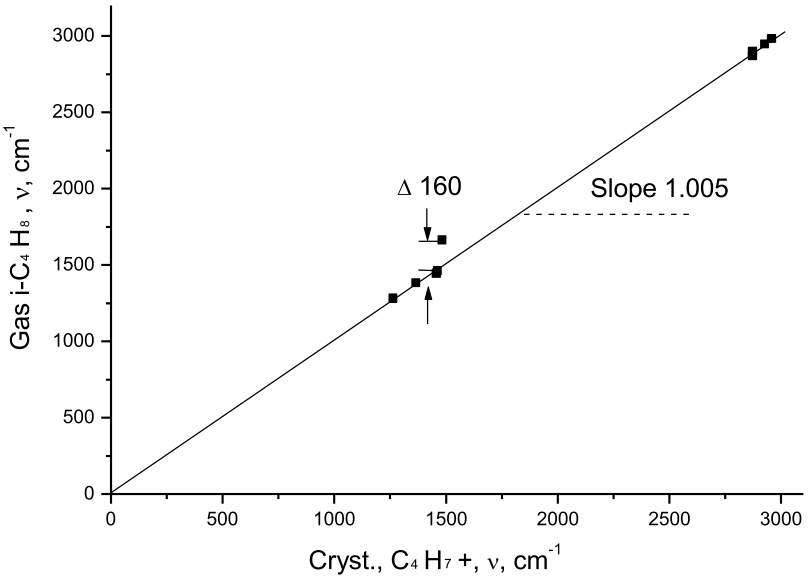

Figure 11. Correlation between experimental frequencies of the isobutylene cation in the crystal salt and experimental frequencies for gaseous isobutylene for vibrations of CH_3 groups and CC bonds of the same type of symmetry (excluding frequencies of $=CH_2$ groups in isobutylene and $=CH^+$ in the cation).

Table 1. Frequencies of CH and C=C Stretch Vibrations and Bent Vibrations of the CH_3 Groups in Experimental IR Spectra of Gaseous Isobutene and of the Isobutenyl Cation in the Crystal Salt in Comparison with Those Calculated at the B3LYP/6-311++G(d,p) and HF/6-311++G(d,p) Levels of Theory

	isobutene, C_4H_8		t-$C_4H_7^+$	
assignment[26]	gas[26]	calcd., DFT	crystal	calcd., HF
νCH_2 as	3088	3207		
νCH_2 s	2980	3127		
νCH^+			[a]	3466
νCH_3 as	2980	3103	2960	3302
νCH_3 as	2944	3052	2930	3286
νCH_3 s	2895, 2867	3010	2874	3195
$\nu C{=}C$	1660	1713	1485	1818
δCH_3 as	1459	1501	1465	1601, 1592
δCH_3 as	1442	1489	1459	1581
δCH_3 s	1379	1409	1368	1509

[a]The band of the $C{-}H^+$ stretch of the crystal sample overlaps with the strong band of νCH of the anion; for the amorphous sample, this frequency is 3040 cm^{-1}.

indicating considerable weakening of hyperconjugation, while the frequencies of the CC stretch actually did not change, but the intensity of their absorption decreased (Figure 4). The spectrum of the crystalline $C_4H_7^+\{Cl_{11}^-\}$ salt includes the bands of CH stretches common for hydrocarbons, not perturbed by hyperconjugation. In addition, the spectrum contains no bands of the CC stretch having one-and-a-half-bond status. Such changes in the spectrum of the $C_4H_7^+$ cation can be caused by an increase in the molecular ordering of the solid phase during its transition to the crystalline phase. These changes in the spectra can be explained as follows.

At the first moment of the interaction of DCMP with $H\{Cl_{11}\}$, ion pairs $C_4H_7^+\{Cl_{11}^-\}$ with shortened ionic bond $=C^+H\cdots\{Cl_{11}^-\}$ are formed (the IR spectrum in Figure 4, red). They are in a highly disordered environment with which the CH_3 groups interact weakly. Therefore, the charge is shifted to the C=C bond and reduces the population of the $2p_z$ orbital of the sp^2 carbon atom. These changes lead to the emergence of strong hyperconjugation: the σ-electron density of CH bonds is brought to the $2p_z$ orbital, thereby contributing to efficient scattering of the positive charge over all H atoms of the cation and partial strengthening of two C−C bonds. Thus, intramolecular stabilization of the cation takes place. Shortly after the formation of $C_4H_7^+\{Cl_{11}^-\}$ is completed, molecular ordering of the amorphous phase increases, enhancing the interaction of the cation with the immediate environment, thereby weakening hyperconjugation (the IR spectrum in Figure 4, green). Finally, in the ordered crystalline phase, the strength of the interaction of the CH_3 groups with neighboring anions leads to a fading of ion pairing (the $=C^+H\cdots\{Cl_{11}^-\}$ distance is only slightly shorter than other $H\cdots\{Cl_{11}^-\}$ distances) and conversion of the salt phase to purely ionic state. The $2p_z$ orbital of such a cation is filled and hyperconjugation disappears, increasing the positive-charge localization on the C=C bond (its stretch frequency decreases further by 70 cm^{-1}, see Figure 4, blue). Therefore, in the crystalline phase, the cation is stabilized due to the intermolecular interaction with the anions of the environment and transfers a portion of its charge to the anions.

These results show how strongly the anionic environment affects the electron density distribution in the cation, changing its IR spectrum. This may be the reason why the quantum-chemical calculations for vinyl cations under vacuum contradict the experimental data concerning the C=C bonds of the cations in the condensed phase: the calculations do not take into account the decisive effect of solvation by the anionic environment.

It was shown here that in vinyl cations with electron-donor alkane- or β-silyl-substituents attached to the C atoms of the C=C bond, the positive charge is effectively distributed over the substituents, and the remaining weakened charge on the C=C bond causes an increase in electron density on this bond as compared with a neutral analogue. This phenomenon is manifested in an increase of the C=C stretch up to 1958/1987 cm^{-1}, which corresponds to the bond order for C=C

https://doi.org/10.1021/acsomega.1c01297
ACS Omega 2021, 6, 15834−15843

markedly higher than 2 (refs 4 and 5) (actually >2.5). The length of the C═C bond shortens (to 1.234 Å), approaching that of the triple C≡C bond.[5] These effects result is in good agreement with density functional calculations.[4] In the present work, the studied vinyl cation $C_4H_7^+$ does not contain donor groups. A positive charge on its C═C bond increases significantly, driving a strong decrease in C═C stretch frequency by 160 cm^{-1}, as compared to neutral isobutene. This finding is inconsistent with the quantum chemical prediction for a bare cation under vacuum. A possible reason for this discrepancy is that a vinyl cation with a high charge on the C═C bond is very susceptible to the influence of the anionic environment. In this case, the experimental spectroscopic properties of such cations in a gas phase should differ significantly from those in the condensed phase, and future experiments will give an answer.

4. CONCLUSIONS

Unsaturated carbocation $C_4H_7^+$ was obtained for the first time in amorphous and crystalline salts with the carborane anion, $CHB_{11}Cl_{11}^-$, and was characterized by X-ray crystallography. Using DCMP as a precursor, the isobutylene isomer $(CH_3)_3C{=}CH^+$ is formed, which is believed to be a thermodynamically least stable $C_4H_7^+$ isomer. The use of other precursors can lead to the formation of other isomers of the $C_4H_7^+$ cation. We will continue our research in this direction.

Electron density distribution and charge dispersion over the isobutylene cation are very sensitive to the immediate environment. In the amorphous phase, in the presence of a significant disorder of the anionic environment, the cation is ionically bonded to the most basic Cl atom of the anion via its ═C−H fragment, on which the "+" charge is mostly concentrated promoting to ion pairing. The charge has a strong effect on the C═C bond, lowering its CC stretch by 105 cm^{-1}, in comparison with neutral isobutylene. Unexpectedly, the $2p_z$ orbital of the central sp^2 C atom seems to be unfilled, and two CH_3 groups take part in strong hyperconjugation, even stronger than that in unsaturated t-Bu^+: the C−H bonds supply their σ-electrons to the $2p_z$ orbital, thereby imparting some π-character to the CC bonds. This effect promotes positive charge dispersion over the cation up to hydrogen atoms of the CH_3 groups, thus increasing its stability. With an increase in molecular ordering of the amorphous phase, the H atoms of the cation more uniformly interact with the surrounding anions, which weakened ion pairing and the hyperconjugation effect (CH stretches is blue-shifted by 86 cm^{-1}). In the ordered crystalline phase, the interaction of the cation with neighboring anions becomes mostly uniform and the ion pairing actually disappears, transforming the salt into a highly ionic state. This leads to disappearance of hyperconjugation. That is, the stabilization of the cation occurs due to the interaction with the anions of the environment and the transfer of a positive charge to them. Such a high sensitivity of the charge distribution over the cation from the nearest environment of the medium is probably the reason why the quantum chemical calculations for the cation under vacuum do not agree with the experimental data for the cation in the condensed phase. The available calculation methods for the condensed phase are also insufficiently developed for the study of such systems or require a lot of computer time for calculations.

The presented results of the study of only one isomer of the $C_4H_7^+$ carbocation, isobutylene, completely agree with the results of subsequent X-ray and IR spectroscopic studies of all the three isomers of the allyl cation $C_3H_5^+$ in its carborane salts,[27] as well as other alkene carbocations, which are currently being studied. Therefore, the features of the properties of the isobutylene carbocation are typical for the entire class of alkene carbocations.

5. EXPERIMENTAL SECTION

5.1. Experimental Methods. All sample handling was carried out in an atmosphere of argon (H_2O, [O_2] < O.5 ppm) in a glove box. Carborane acid, H{Cl_{11}}, was prepared as described previously.[28] It was purified by sublimation at 150−160 °C under a pressure of 10^{-5} Torr on cold Si windows in a specially designed IR cell reactor (a detailed description is given in the Supporting Information). The formed thin translucent layer is sufficient to obtain an intense IR spectrum.

The salt $CH_2Cl\{Cl_{11}\}$ was obtained as previously described:[29] the vapors of dichloromethane (DCM) were injected into the IR cell reactor containing a thin layer of the sublimed acid on the Si windows. The reaction takes place within a few minutes and when the absorption intensity of the CH_2Cl^+ cation reached a maximum, and the absorption of free acid disappeared, the reaction was stopped by the removal of DCM vapors by evacuation. The salts of carbocations under study were obtained by injecting the DCMP vapors into an IR cell with the obtained layer of the $CH_2Cl\{Cl11\}$ salt on its Si windows.

The DCMP from Toronto Research Chemicals Inc. was used without further purification.

The IR spectra were recorded on a Shimadzu IRAffinity-1S spectrometer housed inside the glove box in the 4000−400 cm^{-1} frequency range in transmittance and ATR mode. The spectra were processed in GRAMMS/A1 (7.00) software from Thermo Scientific.

X-ray crystallographic data were obtained by means of a Bruker Kappa Apex II CCD diffractometer using φ, ω scans of narrow (0.5°) frames with Mo Kα radiation (λ = 0.71073 Å) and a graphite monochromator. The structures were solved by direct methods using the SHELX-97 software suite[30] and were refined by the full-matrix least-squares method against all F^2 in anisotropic approximation using SHELXL-2014/7 software.[31] Absorption corrections were applied by the empirical multiscan method in the SADABS software.[32] Hydrogen atoms' positions, except for the H atom at C1K, were calculated via the riding model. The H atom at C1K was located on a difference Fourier map and refined freely. The obtained crystal structure was analyzed for short contacts between nonbonded atoms in PLATON[33] and MERCURY.[34] Crystallographic data and details of the X-ray experiment are listed in Table S1 in the Supporting Information. The structure is formed by crystallographically independent 1/2 part of molecules of the anion and cation. CCDC 2041857 contains the supplementary crystallographic data for this paper. These data can be obtained free of charge via http://www.ccdc.cam.ac.uk/cgi-bin/catreq.cgi or from the Cambridge Crystallographic Data Centre, 12 Union Road, Cambridge CB2 1EZ, UK; fax: (+44) 1223 336 033; or e-mail: deposit@ccdc.cam.ac.uk.

Details of X-ray structural analyses are provided in the Supporting Information.

5.2. Theoretical Calculations. All calculations were performed at the B3LYP[35] /6-311G++(d,p)[36] level of theory

https://doi.org/10.1021/acsomega.1c01297
ACS Omega 2021, 6, 15834−15843

with Grimme dispersion correction,[37] HF, and MP2[38] level theory with an ultrafine integration grid within the framework of the Gaussian 09 package.[39] All cations were calculated at singlet state. When calculating a cation surrounded by 13 argon atoms, a Grimme dispersion correction was used for more accurate calculation van der Waals interaction.

The vibrational frequencies were calculated for all the studied structures, where the optimization converged successfully to the shallow local minima on the potential energy surface, which was confirmed by the absence of negative/imaginary vibrational frequencies.

■ ASSOCIATED CONTENT

Supporting Information

The Supporting Information is available free of charge at https://pubs.acs.org/doi/10.1021/acsomega.1c01297.

Cell reactor design, details of X-ray data, additional IR spectra and IR spectra separated by subtraction, and optimization of the isobutylene cation in an environment simulating a crystal lattice (PDF)

■ AUTHOR INFORMATION

Corresponding Author

Evgenii S. Stoyanov − *Vorozhtsov Novosibirsk Institute of Organic Chemistry SB RAS, Novosibirsk 630090, Russia;* orcid.org/0000-0001-6596-9590; Email: evgenii@nioch.nsc.ru

Authors

Irina Yu. Bagryanskaya − *Vorozhtsov Novosibirsk Institute of Organic Chemistry SB RAS, Novosibirsk 630090, Russia*

Irina V. Stoyanova − *Vorozhtsov Novosibirsk Institute of Organic Chemistry SB RAS, Novosibirsk 630090, Russia*

Complete contact information is available at: https://pubs.acs.org/10.1021/acsomega.1c01297

Notes

The authors declare no competing financial interest.

■ ACKNOWLEDGMENTS

This work was supported by grant # 16-13-10151 from the Russian Science Foundation. The authors thank Viktor Yu. Kovalskii for providing the quantum-chemical calculations. The English language was corrected and certified by shevchuk-editing.com.

■ REFERENCES

(1) Olah, G. A.; Prakash, S. G. K.; Molnar, A.; Sommer, J. *Superacid Chemistry*, 2nd ed.; Wiley: Hoboken, NJ, 2009.

(2) Albrigth, T. A.; Freeman, W. J.; Schweizer, E. E. Magnetic resonance studies. II. Investigation of phosphonium salts containing unsaturated groups by carbon-13 and phosphorus-31 nuclear magnetic resonance. *J. Am. Chem. Soc.* **1975**, *97*, 2946−2960.

(3) Salnikov, G. E.; Genaev, A. M.; Bushmelev, V. A.; Shubin, V. G. Migration of methylethynyl group in a long-lived carbocation. *Org. Biomol. Chem.* **2013**, *11*, 1498−1501.

(4) Müller, T.; Juhasz, M.; Reed, C. A. The X-ray Structure of a Vinyl Cation. *Angew. Chem., Int. Ed.* **2004**, *43*, 1543−1546.

(5) Klaer, A.; Saak, W.; Haase, D.; Müller, T. Molecular Structure of a Cyclopropyl Substituted Vinyl Cation. *J. Am. Chem. Soc.* **2008**, *130*, 14956−14957.

(6) Klaer, A.; Syha, Y.; Nasiri, H. R.; Müller, T. Trisilyl-Substituted Vinyl Cations. *Chem.—Eur. J.* **2009**, *15*, 8414−8423.

(7) Siehl, H.-U. *Dicoordinated Carbocations*; Rappoport, Z., Stang, P., Eds.; Wiley: New York, 1997; pp 189−236.

(8) Siehl, H.-U. *Stable Carbocation Chemistry*; Prakash, G. K. S., Schleyer, P. v. R., Eds.; Wiley: N.-Y., 1997; pp 165−196.

(9) Siehl, H. U.; Kaufmann, F.-P.; Apeloig, Y.; Braude, V.; Danovich, D.; Berndt, A.; Stamatis, N. The First Persistentβ-Silyl-Substituted Vinyl Cation. *Angew. Chem., Int. Ed.* **1991**, *30*, 1479−1482.

(10) Lauvergnat, D.; Hiberty, P. C.; Danovich, D.; Shaik, S. Comparison of C−Cl and Si−Cl Bonds. A Valence Bond Study. *J. Phys. Chem.* **1996**, *100*, 5715−5720.

(11) Sini, G.; Maitre, P.; Hiberty, P. C.; Shaik, S. S. Covalent, ionic and resonating single bonds. *J. Mol. Struct.* **1991**, *229*, 163−188.

(12) Duncan, M. A. Infrared laser spectroscopy of mass-selected carbocations. *J. Phys. Chem. A* **2012**, *116*, 11477−11491.

(13) Douberly, G. E.; Ricks, A. M.; Schleyer, P. v. R.; Duncan, M. A. Infrared spectroscopy of gas phase C3H5+: The allyl and 2-propenyl cations. *J. Chem. Phys.* **2008**, *128*, 021102.

(14) Vogel, P. *Carbocation Chemistry*; Elsevier: Amsterdam, 1985; p 173.

(15) Buzek, P.; Schleyer, P. R.; Vančik, H.; Mihalic, Z.; Gauss, J. Generation of the parent allyl cation in a superacid cryogenic matrix. *Angew. Chem., Int. Ed.* **1994**, *33*, 448−451.

(16) Mišić, V.; Piech, K.; Bally, T. Carbocations generated under stable conditions by ionization of matrix-isolated radicals: The allyl and benzyl cations. *J. Am. Chem. Soc.* **2013**, *135*, 8625−8631.

(17) Reed, C. A. Carborane acids. New "strong yet gentle" acids for organic and inorganic chemistry. *Chem. Commun.* **2005**, 1669−1677.

(18) Stoyanov, E. S.; Hoffmann, S. P.; Juhasz, M.; Reed, C. A. The Structure of the Strongest Brønsted Acid: The Carborane Acid H(CHB11Cl11). *J. Am. Chem. Soc.* **2006**, *128*, 3160−3161.

(19) Crowder, G. A.; Richardson, M. T. Vibrational analysis of 1,2-dichloro-2-methylpropane and 1,2-dibromo-2-methylpropane. *J. Mol. Struct.* **1982**, *78*, 229−246.

(20) Rowland, R. S.; Taylor, R. Intermolecular nonbonded contact distances in organic crystal structures: Comparison with distances expected from van der Waals radii. *J. Phys. Chem.* **1996**, *100*, 7384−7391.

(21) Stoyanov, E. S.; Gomes, G. d. P. tert-Butyl Carbocation in Condensed Phases: Stabilization via Hyperconjugation, Polarization, and Hydrogen Bonding. *J. Phys. Chem. A* **2015**, *119*, 8619−8629.

(22) Stoyanov, E. S.; Malykhin, S. E. Carbon monoxide protonation in condensed phases and bonding to surface superacidic Brønsted centers. *Phys. Chem. Chem. Phys.* **2016**, *18*, 4871−4880.

(23) Schultz, J. C.; Houle, F. A.; Beauchamp, J. L. Photoelectron spectroscopy of isomeric C_4H_7 radicals. Implications for the thermochemistry and structures of the radicals and their corresponding carbonium ions. *J. Am. Chem. Soc.* **1984**, *106*, 7336−7347.

(24) Lias, S. G.; Ausloos, P. Structures and heats of formation of $C_4H_7^+$ ions in the gas phase. *Int. J. Mass Spectrom. Ion Processes* **1987**, *81*, 165−181.

(25) Traeger, J. C. A photoionization study of $[C_4H_7]^+$ ions in the gas phase. *Org. Mass Spectrom.* **1989**, *24*, 559−564.

(26) Sverdlov, L. M.; Kovner, M. A.; Krainov, E. P. *Vibrational Spectra of Polyatomic Molecules*; Nauka: Moscow, 1970.

(27) Stoyanov, E. S.; Bagryanskaya, I. Yu.; Stoyanova, I. V. Isomers of Allyl Carbocation $C_3H_5^+$ in Solid Salts: Infrared Spectra and Structures; Submitted for publication.

(28) Juhasz, M.; Hoffmann, S.; Stoyanov, E.; Kim, K.-C.; Reed, C. A. The strongest isolable acid. *Angew. Chem., Int. Ed.* **2004**, *43*, 5352−5355.

(29) Stoyanov, E. S. The salts of chloronium ions R-Cl+-R (R = CH_3 or CH_2Cl): formation, thermal stability, and interaction with chloromethanes. *Phys. Chem. Chem. Phys.* **2016**, *18*, 12896−12904.

(30) Sheldrick, G. M. *SHELX-97, Programs for Crystal Structure Analysis (Release 97-2)*; University of Göttingen: Germany, 1997.

(31) Sheldrick, G. M. Crystal structure refinement withSHELXL. *Acta Crystallogr.* **2015**, *71*, 3−8.

(32) *SADABS*, v. 2008-1; Bruker AXS: Madison, WI, USA, 2008.

(33) (a) Spek, A. L. *PLATON, A Multipurpose Crystallographic Tool (Version 10M)*; Utrecht University: Utrecht, The Netherlands, 2003. (b) Spek, A. L. Single-crystal structure validation with the programPLATON. *J. Appl. Crystallogr.* **2003**, *36*, 7−13.
(34) Macrae, C. F.; Edgington, P. R.; McCabe, P.; Pidcock, E.; Shields, G. P.; Taylor, R.; Towler, M.; van de Streek, J. Mercury: visualization and analysis of crystal structures. *J. Appl. Crystallogr.* **2006**, *39*, 453−457.
(35) Becke, A. D. Density-functional thermochemistry. III. The role of exact exchange. *J. Chem. Phys.* **1993**, *98*, 5648−5652.
(36) (a) McLean, A. D.; Chandler, G. S. Contracted Gaussian basis sets for molecular calculations. I. Second row atoms, Z=11-18. *J. Chem. Phys.* **1980**, *72*, 5639−5648. (b) Raghavachari, K.; Binkley, J. S.; Seeger, R.; Pople, J. A. Self-Consistent Molecular Orbital Methods. 20. Basis set for correlated wave-functions. *J. Chem. Phys.* **1980**, *72*, 650−654. (c) Clark, T.; Chandrasekhar, J.; Spitznagel, G. n. W.; Schleyer, P. v. R. Efficient diffuse function-augmented basis sets for anion calculations. III. The 3-21+G basis set for first-row elements, Li-F. *J. Comp. Chem.* **1983**, *4*, 294−301. (d) Frisch, M. J.; Pople, J. A.; Binkley, J. S. Self-consistent molecular orbital methods 25. Supplementary functions for Gaussian basis sets. *J. Chem. Phys.* **1984**, *80*, 3265−3269.
(37) Grimme, S.; Antony, J.; Ehrlich, S.; Krieg, H. A consistent and accurate ab initio parametrization of density functional dispersion correction (DFT-D) for the 94 elements H-Pu. *J. Chem. Phys.* **2010**, *132*, 154104.
(38) (a) Frisch, M. J.; Head-Gordon, M.; Pople, J. A. A direct MP2 gradient method. *Chem. Phys. Lett.* **1990**, *166*, 275−280. (b) Frisch, M. J.; Head-Gordon, M.; Pople, J. A. Semi-direct algorithms for the MP2 energy and gradient. *Chem. Phys. Lett.* **1990**, *166*, 281−289. (c) Head-Gordon, M.; Pople, J. A.; Frisch, M. J. MP2 energy evaluation by direct methods. *Chem. Phys. Lett.* **1988**, *153*, 503−506. (d) Saebø, S.; Almlöf, J. Avoiding the integral storage bottleneck in LCAO calculations of electron correlation. *Chem. Phys. Lett.* **1989**, *154*, 83−89. (e) Head-Gordon, M.; Head-Gordon, T. Analytic MP2 frequencies without fifth-order storage. Theory and application to bifurcated hydrogen bonds in the water hexamer. *Chem. Phys. Lett.* **1994**, *220*, 122−128.
(39) Frisch, M. J.; Trucks, G. W.; Schlegel, H. B.; Scuseria, G. E.; Robb, M. A.; Cheeseman, J. R.; Scalmani, G.; Barone, V.; Mennucci, B.; Petersson, G. A.; Nakatsuji, H.; Caricato, M.; Li, X.; Hratchian, H. P.; Izmaylov, A. F.; Bloino, J.; Zheng, G.; Sonnenberg, J. L.; Hada, M.; Ehara, M.; Toyota, K.; Fukuda, R.; Hasegawa, J.; Ishida, M.; Nakajima, T.; Honda, Y.; Kitao, O.; Nakai, H.; Vreven, T.; Montgomery, J. A.; Peralta, J. E.; Ogliaro, F.; Bearpark, M.; Heyd, J. J.; Brothers, E.; Kudin, K. N.; Staroverov, V. N.; Kobayashi, R.; Normand, J.; Raghavachari, K.; Rendell, A.; Burant, J. C.; Iyengar, S. S.; Tomasi, J.; Cossi, M.; Rega, N.; Millam, J. M.; Klene, M.; Knox, J. E.; Cross, J. B.; Bakken, V.; Adamo, C.; Jaramillo, J.; Gomperts, R.; Stratmann, R. E.; Yazyev, O.; Austin, A. J.; Cammi, R.; Pomelli, C.; Ochterski, J. W.; Martin, R. L.; Morokuma, K.; Zakrzewski, V. G.; Voth, G. A.; Salvador, P.; Dannenberg, J. J.; Dapprich, S.; Daniels, A. D.; Farkas, Ö.; Foresman, J. B.; Ortiz, J. V.; Cioslowski, J.; Fox, D. J. *Gaussian 09*; Gaussian, Inc.: Wallingford CT, 2009.

https://doi.org/10.1021/acsomega.1c01297
ACS Omega 2021, 6, 15834−15843